

An order-of-magnitude estimate of the current uplift-rates in Switzerland caused by the Würm Alpine deglaciation

Autor(en): **Gudmundsson, G. Hilmar**

Objektyp: **Article**

Zeitschrift: **Eclogae Geologicae Helvetiae**

Band (Jahr): **87 (1994)**

Heft 2: **Pollution and pollutant transport in the geosphere, a major environmental issue : symposium held during the 173rd annual meeting of the Swiss Academy of Natural Sciences**

PDF erstellt am: **27.04.2024**

Persistenter Link: <https://doi.org/10.5169/seals-167470>

Nutzungsbedingungen

Die ETH-Bibliothek ist Anbieterin der digitalisierten Zeitschriften. Sie besitzt keine Urheberrechte an den Inhalten der Zeitschriften. Die Rechte liegen in der Regel bei den Herausgebern.

Die auf der Plattform e-periodica veröffentlichten Dokumente stehen für nicht-kommerzielle Zwecke in Lehre und Forschung sowie für die private Nutzung frei zur Verfügung. Einzelne Dateien oder Ausdrucke aus diesem Angebot können zusammen mit diesen Nutzungsbedingungen und den korrekten Herkunftsbezeichnungen weitergegeben werden.

Das Veröffentlichen von Bildern in Print- und Online-Publikationen ist nur mit vorheriger Genehmigung der Rechteinhaber erlaubt. Die systematische Speicherung von Teilen des elektronischen Angebots auf anderen Servern bedarf ebenfalls des schriftlichen Einverständnisses der Rechteinhaber.

Haftungsausschluss

Alle Angaben erfolgen ohne Gewähr für Vollständigkeit oder Richtigkeit. Es wird keine Haftung übernommen für Schäden durch die Verwendung von Informationen aus diesem Online-Angebot oder durch das Fehlen von Informationen. Dies gilt auch für Inhalte Dritter, die über dieses Angebot zugänglich sind.

An order-of-magnitude estimate of the current uplift-rates in Switzerland caused by the Würm Alpine deglaciation

G. HILMAR GUDMUNDSSON¹

Key words: Uplift-rates, geodynamics, Würm deglaciation, effective elastic thickness, mantle viscosity

ABSTRACT

A viscoelastic model of the crust and the mantle is used to give an order of magnitude estimate of the contribution of glacial isostatic adjustment caused by the Late Würm Alpine deglaciation to the currently observed uplift-rate of the Swiss Alps. Relaxation times are based on a realistic rheological model and not simply assumed. Calculated uplift-rates depend critically on the effective elastic thickness (EET) of the crust-mantle system as well as on the average linear viscosity of the mantle. An important connection is thereby established between the rheology of the Alpine region, the glaciation of the Late Würm and the magnitude of the glacial isostatic rebound. For a range of model parameters in agreement with geological and geophysical findings, calculated uplift-rates are of the same magnitude as measured rates. At this level of modelling the possibility cannot be ruled out that some or even a large part of the currently observed uplift is caused by glacial isostatic rebound.

ZUSAMMENFASSUNG

Mit Hilfe eines viskoelastischen Modells der Kruste und des Mantels wird die Grössenordnung des isostatischen Ausgleichsprozesses abgeschätzt, der durch den spätwürmzeitlichen Zerfall der Alpengletscher in Gang gesetzt wurde. Relaxationszeiten werden anhand eines realistischen rheologischen Modells berechnet. Die berechneten Hebungsdaten hängen stark von der effektiven elastischen Plattenmächtigkeit des Krusten-Mantel-Systems und der mittleren linearen Viskosität des Mantels ab. Damit ist ein Zusammenhang zwischen der Rheologie der Alpenregion, der spätwürmzeitlichen Vergletscherung und der Magnitude des glazialen isostatischen Ausgleichsprozesses hergestellt. Für einen Bereich der Modellparameter, der mit geologischen wie geophysikalischen Ergebnissen im Einklang steht, resultieren Hebungsdaten von derselben Grössenordnung wie die beobachteten. Auf dieser Stufe der Modellierung kann daher die Möglichkeit nicht ausgeschlossen werden, dass ein erheblicher Anteil der heute gemessenen Hebungsdaten auf glazial bedingte isostatische Ausgleichsprozesse zurückzuführen ist.

1 Introduction

Geodetic measurements carried out by the Swiss Federal Office of Topography (Funk and Gubler 1980; Gubler et al. 1984) show a relative uplift-rate of the Alps with respect to the northern Alpine foreland of the order of 1 mm/a.

The cause of this uplift is not known but it has been argued that it is an expression of the ongoing tectonic processes at the contact zone between the Eurasian and the African plates, and the isostatic rebound due to excessive depths of the Mohorovičić-discontinuity

¹ VAW-ETHZ, Gloriastrasse 37/39, CH-8092 Zürich

that are not isostatically compensated by the topographic load of the Alps (Kahle et al. 1980; Gubler et al. 1981). Geodynamical models of the Alpine region have, however, shown that the presence of a lithospheric root known to be situated below the Alps (Mueller 1989; Spakman 1990) is crucial to give results comparable to the velocity pattern measured at the surface (Werner 1985; Gudmundsson 1989). The upward velocity component due to the thicker than average crust is not only compensated for by the topography but also by density disturbances of the asthenosphere. The magnitude of the combined effect can only be estimated if detailed information is available on the spatial extension of the lithospheric root (or roots), its density contrast, as well as the density contrast at the M-discontinuity, and the rheological behavior of the upper mantle. This information is not likely to be available in the nearest future.

Attempts to calculate three-dimensional isostatic anomalies (Klingel  and Kissling 1982) and correlate them with the observed uplift pattern have given valuable insight into the geodynamics of the Alpine region but cannot, partly because a compensation level above the depth range of the lithospheric root was used, give quantitative answers to the question of the relative importance of vertical movements due to density disturbances within the crust and the mantle and those due to postglacial isostatic rebound.

Various geological observations have shown unequivocally that the Alps have experienced a complicated pattern of subsidence and uplift since the start of the main phase of the Alpine deformation in the early Late Cretaceous. Reconstruction of the uplift history based on fission-track ages has for example shown significant temporal and spatial changes with time (Hurford et al. 1989) and there seems to be no reason to assume that this uplift process caused by tectonic movements is not operating today. Exact comparison of actual and reconstructed uplift-rate is however difficult due to the limited time resolution of the fission-track method and although some general agreement has been found the results presented do not rule out the possibility that some of the present-day uplift is a result of the melting of the Quaternary glaciers (Schaer et al. 1975).

One obvious possible cause of uplift is glacial isostatic rebound. Schaer and Jeanrichard (1974), in a classic paper, compared the situation in the Swiss Alps with the one of Lake Mead (Arizona–Nevada), the late Pleistocene pluvial Lake Bonneville (Utah–Nevada) and Fennoscandia, and obtained values for the viscous relaxation time and concluded that it is “highly probable [that] the deformations recorded today stem from another source”, i. e. that they are not caused by glacial isostatic rebound.

Attempts to correlate the extension of glaciation with measured spatial uplift pattern have so far been inconclusive (J ckli 1957, 105–106; Schneider 1976, page 84–94; Hantke 1980, page 394–396). Qualitative observations in favour and against considerable isostatic rebound caused by the melting of the Alpine W rm glaciation can be found.

Some quantitative approach is needed to clarify these matters. Strangely enough no numerical estimates of the possible uplift-rate, using models equivalent to those applied to the same physical phenomenon in other areas of the world, have been done for the European Alpine region. The relaxation times used by Schaer and Jeanrichard were an input and not an output of some rheological model of the earth. The main difference to their work is that the relaxation spectrum is here an output and not an input of a rheological model. The rheological model chosen is equivalent to models that have been used successfully for areas including Lake Bonneville as well as Fennoscandia (Nakiboglu and Lambeck 1982; Officer et al. 1988) and Iceland (Sigmundsson 1990). It consists of a thick

elastic plate overlying a viscous mantle. The parameters entering the model are in accordance with current knowledge about the value of EET for the European Alps and are discussed in Sec. 3.2.

The uplift resulting from a loading history corresponding in broad terms to the extent of the Late Würm glaciation is calculated. Thereby a connection is established between the possible rheological properties of the European alpine system, the measured uplift-rate and the amount of glaciation during Late Würm. This connection is important in itself and can for example put restraint on the viscosity profile used in geodynamic models where surface velocities caused by density disturbances within the crust and mantle are calculated.

2 Alpine glaciation during Late Würm

The history of the last Alpine glaciation is known in some detail (Hantke 1980; Haeberli and Penz 1985). There were at least two, but possibly more, major periods of glaciation during Würm. Only the latest one (Late Würm) is of relevance to this study. Between 60,000 and 28,000 B.P. there are indications of an ice-free Alpine Foreland (Schluchter 1991). In this period the glaciers were limited to the Alpine region itself. Around 25,000 B.P. a massive ice build-up started which reached its maximum at 20,000–18,000 B.P. at which time about 126,000 km² were covered with ice. The maximum extent of the ice cover can be seen in Figure 1. The thickness of the ice varied greatly. The alpine valleys were

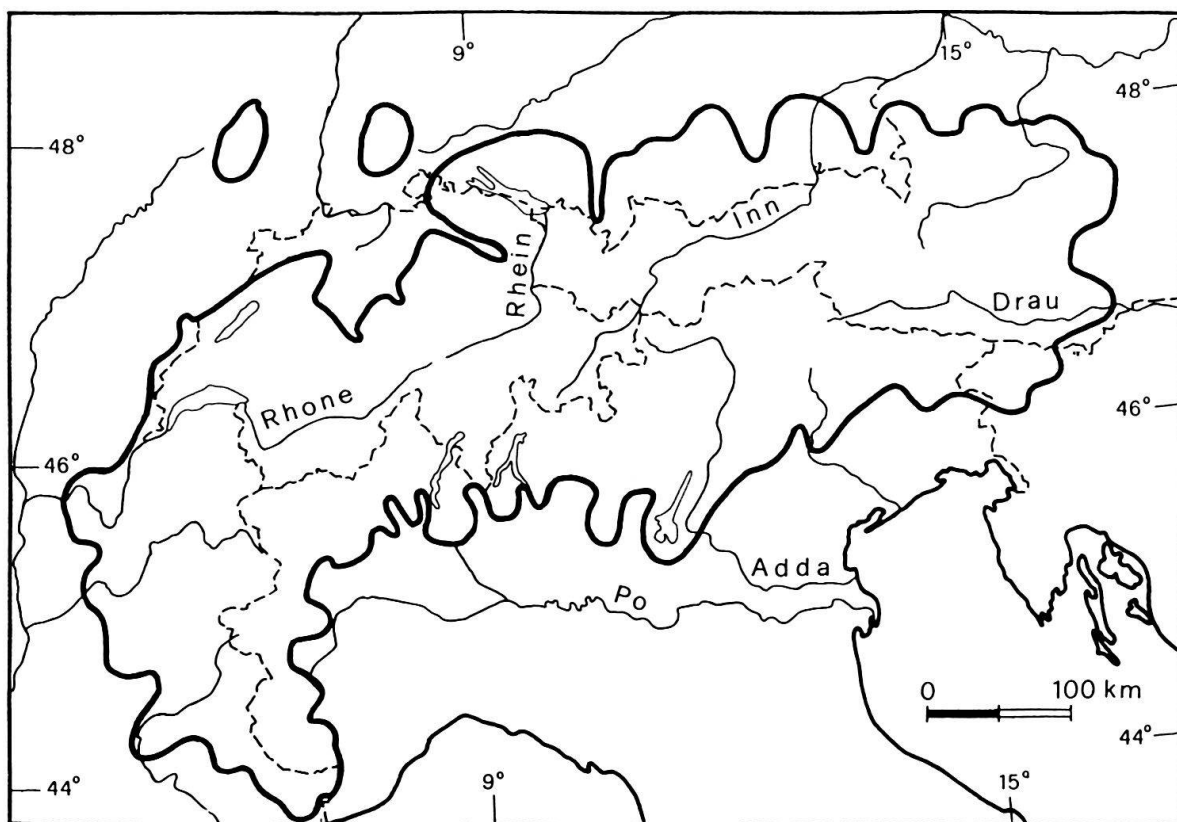


Fig. 1. The maximum extent of the alpine glaciation during Late Würm around 20,000–18,000 B.P. Only approximative boundaries are shown. Based on Hantke (1980), Haeberli and Penz (1985); de Beaulieu et al. (1991) and Jäckli (1970).

covered with up to 1500 m thick ice, but in the Alpine Foreland the maximum thickness was somewhere around 300 to 400 meters (Keller and Krayss 1991; Dricot et al. 1991; Haeberli and Schlüchter 1987). At about 13,000 B.P. the glaciers had retreated and were again limited to the Alps. At around 10,000 B.P. the Würm glaciation ended. A look at Table 1 shows how much smaller in extent and volume the Alpine glaciation was com-

Table 1. Basic Data on Laurentide (Late Wisconsin), Fennoscandia (Late Weichselian and Y. Dryas) Ice Sheets and the Alpine glaciation (Late Würm)

	Alps	Laurentide	Fennoscandia
Length, km	200	2500	2250
Width, km	600	4000	1350
Mean thickness, km	0.3 to 0.4	3.5	2.4
Volume, 10^6 km^3	0.04	32	7.3
Effective radius (R), km	200	1625	900
Start of buildup, ka B.P.	25	35	25
Glaciation maximum, ka B.P.	21 to 18	20 to 18	20 to 18
End of glaciation, ka B.P.	13 to 11	6.5	8.5
D/R	0.05 to 0.33	0.006 to 0.05	0.01 to 0.05

The values are average ones. Lengths and widths refer to maximum extent. Estimate of the mean thickness of the Alpine glaciation is difficult since it varied highly not only in time but also in space. It is possible the maximum ice extension in the French Alps did not take place during Late Würm (de Beaulieu et al. 1991). Because of the Cordilleran ice the N-America glaciation was even somewhat larger than the number indicates for the Laurentide ice sheet. The numbers are based on Dawson (1992), de Beaulieu et al. (1991), Schlüchter (1991), Officer et al. (1988). $D = EET$ = effective thickness of the elastic plate (see Table 2).

pared to the Laurentide and the Fennoscandia Ice Sheets. The glacio-isostatic uplift will therefore be much smaller. In Fennoscandia maximum current uplift-rates are 9 mm/a in the northern part of the Gulf of Bothnia. The corresponding value for Switzerland is 1.7 mm/a which is found close to Chur and refers to Aarburg (Gubler et al. 1992) that is close to the border of the maximum glaciation. There is no doubt that the disappearance of the Late Würm glaciers did cause some vertical movements at the surface and it is interesting in this context that there is evidence of faulting during Holocene at the Rhine-Rhône-Line that can most easily be explained as a result of an isostatic rebound caused by the disappearance of the last Ice Age glaciers, that in this region had great thicknesses (Eckardt et al. 1983). For a quantitative assessment of the isostatic effect of these glaciers, however, a model calculation is needed that simulates the viscoelastic response of the Earth to forces acting over time scales of 10^3 – 10^4 years.

3 Half-space earth model

To estimate the rebound of the crust following the glacial unloading of the Late Würm glaciers it is assumed that the rheological behavior of the upper mantle can be sufficiently well approximated by a model consisting of a Newtonian viscous half-space overlayed by an elastic layer. This assumption is justified by the success of equivalent models that have for example been applied to the same physical phenomenon in Laurentia, Fennoscandia, Iceland and Lake Bonneville.

To get an estimate of the magnitude of the uplifting a cylinder-symmetrical model can be used although the shape of the Late Würm glacier was far from being cylindrical. Calculated values can therefore not be directly compared with the observed spatial distribution of uplifting – but to the overall magnitude of the process.

3.1 Theoretical background

The theoretical formulations for glacio-isostatic adjustment can be found in Cathles (1975). Recently Sigmundsson (1990) has given an excellent account of the mechanical response of a thick plate overlying a viscous half-space to a symmetric cylindrical loading at the surface.

The vertical displacement u_z as a function of the distance r , from the center of the loading and the time t since unloading is given by:

$$u_z(r, t) = \int_0^\infty \bar{\sigma}_{zz}(\beta_1 + \beta_2(1 - e^{-t/\tau})) J_0(kr) k dk \quad (1)$$

where J_0 is the Bessel function of order zero, and β_1 and β_2 are functions of: the thickness of the elastic plate D , the Lamé's parameter μ , and the density of the viscous half space ρ_v .² k is the wavenumber, η the viscosity of the half space and g the gravitational acceleration. $\bar{\sigma}_{zz}$ is the zero order Hankel transformation of the vertical stress σ_{zz} resulting from the loading

$$\bar{\sigma}_{zz}(k) = \int_0^\infty \sigma_{zz}(r) J_0(kr) r dr \quad (2)$$

The function β_1 and β_2 are given by:

$$\beta_1 = \frac{kD - cs}{2\mu k (c^2 + k^2 D^2)} \quad (3)$$

and

$$\beta_2 = - \frac{1 + \frac{\rho_v g}{2\mu k} \frac{s^2}{(cs + kD)}}{\rho_v g \left(1 + \frac{2\mu k}{\rho_v g} \frac{(s^2 - k^2 D^2)}{(cs + kD)}\right)} + \frac{cs - kD}{2\mu k (c^2 + k^2 D^2)} \quad (4)$$

where the abbreviations:

$$s = \sinh(kD) \quad \text{and} \quad c = \cosh(kD) \quad (5)$$

have been used. The relaxation time (t_r) is given by:

$$t_r = \frac{2\eta k D}{\rho_v g D + 2\mu k D \frac{s - kD e^{-kD}}{c + kD e^{-kD}}} \quad (6)$$

² In mathematical equations the symbol D is used for the effective thickness of the elastic plate. In text the abbreviation EET is used.

For a loading with a mean radius R , mean height d , and ice density ρ_i the integral (2) can be calculated and inserted into (1) giving

$$u_z(r, t) = R\rho_i g d \int_0^\infty (\beta_1 + \beta_2(1 - e^{-t/t_r})) J_1(kR) J_0(kr) dk \quad (7)$$

At the center of the loading (where $r = 0$), $J_0(kr)$ is equal to one and the largest contribution to the integral in (7) will be where $J_1(kR)$ obtains its first maximum, or at $kR \approx 1.84$.³ The variations of β_1 , β_2 and t_r as functions of the product kD are depicted in Figure 2. Especially the range around $kD = 1.84 \times D/R$ is interesting since it gives the largest contribution to the integral in (7). Let α be this range of kD values. For the Alpine Region, R can be taken to be from 150 to 200 km and D is somewhere between 10 to 50 km, which gives $\alpha_A = [0.09, 0.6]$ where subscript A refers to the Alpine glaciation. Corresponding ranges for Fennoscandia and the Laurentide ice sheets are: $\alpha_F = [0.02, 0.1]$ and

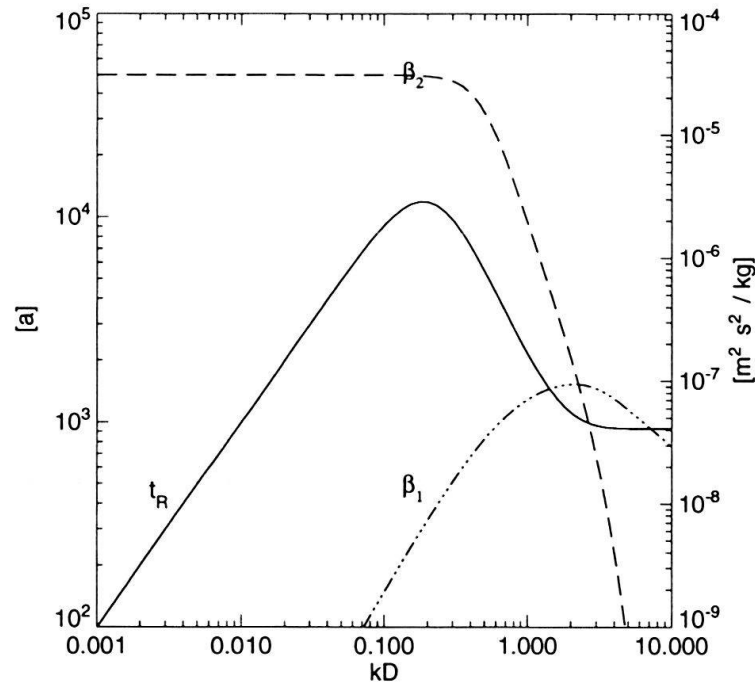


Fig. 2. The relaxation time, t_r , and the functions β_1 and β_2 as functions of kD . The left y-Axis relates to t_r and the right one to β_1 and β_2 . The following values for the relevant parameters were used: $\mu = 3.4 \times 10^{10}$ Pa, $D = 30$ km, $\eta = 10^{21}$ Pa s, $\rho_v = 3250$ kg/m³, and $g = 9.81$ m/s². The peak of the t_r -curve is due to the response of the elastic plate; it can be considered to be a natural dividing point between long and short wavelengths; the long ones having kD -values which lie to the left of the peak and the short ones having kD -values which lie to the right of the maximum of the relaxation curve. For long wavelengths t_r is given by $2\eta k / \rho_v g$, which is the relaxation time for a viscous half space. As explained in the text, the dimensions of the Late Würm Alpine glaciation were such that the range around the t_r peak, where the function β_1 and β_2 also show some interesting behavior, gives the largest contribution to integral (7). This is the reason why the value of the effective elastic thickness ($D = EET$) is so important for the calculated uplift-rate.

³ $J_1(x)$ has a maximum at $x \approx 1.84$ (the maximum is given by $\sqrt{2/(\pi x)}$ and is zero at $x = 0$ and $x \approx 3.83$).

Table 2. Values for the effective elastic thickness of the lithosphere

Area	EET [km]	Method	Author
eastern Alps	50	flexure behavior	Karner and Watts (1983)
western Alps	25	flexure behavior	Karner and Watts (1983)
Appennines	10–20	flexure behavior	Royden (1988)
Aar and Gotthard	10–20	rheology estimate	Cloetingh and Banda (1992)
Swiss molasse	20–35	rheology estimate	Cloetingh and Banda (1992)
Jura	20–35	rheology estimate	Cloetingh and Banda (1992)
Fennoscandia	< 50	shoreline tilting	Fjeldskaar and Cathles (1991)
Lake Bonneville	< 30	uplift	Nakiboglu and Lambeck (1982)

$\alpha_L = [0.01, 0.1]$ respectively, where values for D , from Table 2 have been used. The maximum of $t_r = 2\eta k / \rho_v g$. The position of the maximum of t_r marks a natural distinction between short wavelengths, where the response to loading is mostly determined through the properties of the elastic plate, and long wavelengths where the viscosity is the crucial parameter. If the ratio of D/R is such that the range of kD -values which give the largest contribution to the integral in (7) is around the maximum of t_r , the elastic as well as the viscous properties will be important. This means that the calculated uplift will strongly depend on η as well as D .

Differentiating t_r given by (6) with respect to $\chi = kD$, setting equal to zero and solving for D gives:

$$\frac{Dgd}{2\rho_v\mu} = \frac{2\chi^3}{c^2\chi + 2\chi e^{-\chi}c + \chi^2 e^{-2\chi}} \quad (8)$$

It is worth noticing that the maximum of t_r does not depend on η . Inspection of Eq. (8) shows that the maximum of t_r moves to higher kD -values as D increases, but remains close to the range of kD -values given by α_A . This means that the calculated uplift will be strongly dependent on the exact value of D . The effect of the last global glaciation on the uplift-rate within the Swiss alpine region can therefore not be estimated without accounting for the elastic properties of the lithosphere. On the other hand, an independent estimate of the glacial isostatic adjustment could be used to fix the value of D . It is also clear that the relaxation times of the Alpine region cannot be estimated by using directly relaxation times obtained from regions where the D/R ratio is not the same, as in Fennoscandia. The t_r -spectrum depends critically on the existence of the elastic plate and should be assessed in terms of a rheological model.

3.2 Model parameters

Five rheological parameters define the model. For the elastic layer the Lamé's parameters μ and λ are needed. It is assumed that the elastic layer is incompressible which is, for the problem considered, an excellent approximation and gives $\lambda = \infty$. Using $\mu = \nu_s^2 \rho$,

where v_s is the shear wave velocity and ρ the specific density, gives $\mu \approx 3.4 \times 10^{10}$ Pa, where $v_s = 3.5$ km/s and $\rho_c = 2.81$ g/cm³ have been used as average values for the crust. The thickness of the elastic layer, which can be considered to be the effective elastic thickness of the lithosphere (EET), is as said before an important parameter. Its value is not well known. Calculations of the present rate of uplift in Fennoscandia and N-America do not give an accurate estimate of the value of EET, and even if that were the case the values so obtained could hardly be used for the European Alpine system due to great differences in geology and tectonic settings. The stress field itself can, for example, influence the apparent effective elastic thickness in the presence of a ductile zone in the lower crust (McNutt et al. 1988).

There have been few attempts to estimate the thickness of the EET in the Alps. Table 2 gives a summary of some of the results obtained so far. It can be assumed that EET has a thickness in the range of 10 to 50 km.

For the viscous half-space two parameters are needed: the mean density (ρ_v) and the viscosity (η). For the mean density a value of $\rho_v = 3.25$ g/cm³ was used which corresponds to a mean density of the upper mantle. For EET values smaller than the average crust thickness one could argue that the density of the crust (ρ_c) should be used instead of the density of the mantle. By looking at Eq. (7) one sees that in the long wavelength limit $\beta_1 = -1/\rho_v g$, and that $\beta_2 = 0$, so that u_z as well as \dot{u}_z will be inversely proportional to ρ_v . In the small wavelength limit u_z does not depend on ρ_v . The effect of using ρ_c instead of ρ_m is therefore at most proportional to the ratio ρ_m/ρ_c , can easily be estimated and does not affect the order of magnitude calculation.

There is a general agreement that the average effective viscosity of the mantle is $\sim 1 \times 10^{21}$ Pa s (Karato and Wu 1993). Whether the adjustment is an upper mantle process or a whole mantle process is of no relevance here, since the difference will only be noticeable for the peripheral subsidence zone.

Among the model parameters the viscosity (η) and EET (D) are the only ones that are weakly constrained and have a large effect on the calculated uplift-rate. It is therefore necessary to calculate all quantities of interest for a reasonable range of η and D values.

4 Results

In Figure 3 calculated uplift-rates at the position of the center of the ice-cover ($r = 0$) 13,000 years after its disintegration are depicted, as a function of the viscosity and the EET. Following values were used: $d = 250$ m, $R = 150$ km, $\rho_i = 920$ kg/m³. Notice that the uplift as well as the uplift-rate depends, according to Eq. (7), linearly on the mean ice thickness d . A value of 250 m for d was chosen rather arbitrarily as a reference value. A different value for d will have an easily comprehensible effect on the calculated uplift-rate. The values chosen should represent a rather conservative estimate; the correct values of R and d are expected to be somewhat larger in reality than assumed. The loading history $h(r, t)$, used for Figure 3 was:

$$h(r, t) = \begin{cases} \rho_i g d (1 - H(t - t_1)) & , \text{ if } 0 \leq r \leq R; \\ 0 & , \text{ otherwise.} \end{cases} \quad (9)$$

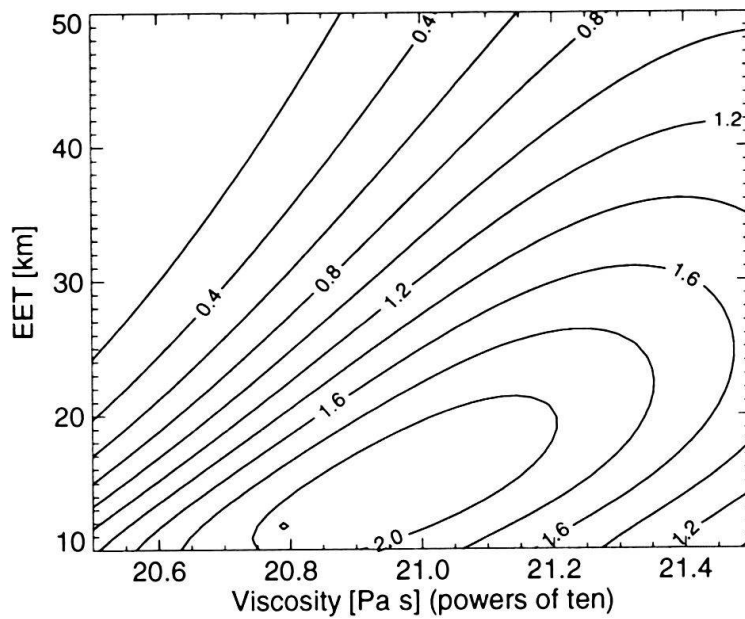


Fig. 3. Uplift-rate in mm/a as a function of mantle viscosity η , and effective elastic thickness (EET). The uplift-rate shown is the difference between the uplift-rate at the center of the hypothetical ice-over and a point 200 km away from the center, 13 ka after the ice-cover has disappeared. The radius of the ice-cover was 150 km and its thickness 250 m. No corrections were applied for the finite duration of the ice loading. Contour intervals are 0.2 mm/a.

where H is the Heaviside unit step function and $t_1 = -13,000$ years. Thus the load is applied at $t = \infty$ until $t = 13,000$ years BP. The importance of finite duration of the loading can be seen in Figure 4 where all parameters are the same as for Figure 3 except the loading history which is given by:

$$h(r, t) = \begin{cases} \rho_i g d (H(t - t_0) - H(t - t_1)), & \text{if } 0 \leq r \leq R; \\ 0, & \text{otherwise.} \end{cases} \quad (10)$$

The load is applied instantaneously at time $t = t_0$, remains constant for $t_0 < t < t_1$, and is suddenly removed at time $t = t_1$. The values for t_0 and t_1 where: $t_1 - t_0 = 10$ ka, and $t_1 = -13$ ka BP. This load is considerably less than the one that Schaer and Jeanrichard used, and is as already explained most likely to be too small. Larger loads will cause higher uplift-rates. Comparison of Figure 3 with Figure 4 shows that the finite duration of the load changes the values obtained by at most a factor of two. The order of magnitude estimate is therefore the same and does not depend critically on the exact timing of the buildup of the glaciers.

A conspicuous feature of Figures 3 and 4 is that the uplift-rates reach a maximum for certain values of η and D , and that for a given effective elastic thickness two different values of η can give the same uplift-rate. Conversely for some value of D the same uplift-rate can correspond to two different η values.

The reason for this behaviour is that if the relaxation-times are short as compared to the time since ice disintegration, which is the case for small viscosity values, the glacial isostatic rebounding has for the most part taken place on early stage, leading to small or

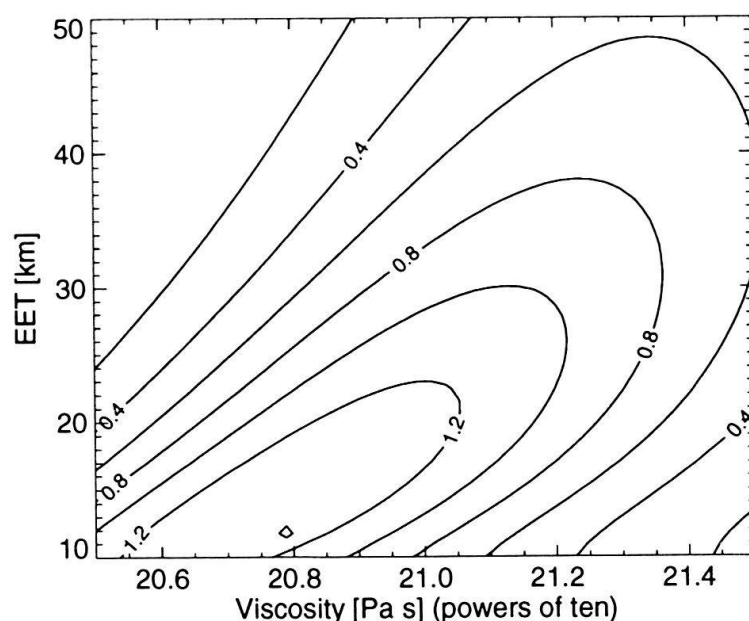


Fig. 4. Uplift-rate in mm/a as a function of mantle viscosity η , and effective elastic thickness for a finite duration of loading.

The uplift-rate shown is the difference between the uplift-rate at the center of the hypothetical ice-cover and a point 200 km away from the center, 13 ka after the ice-cover has disappeared. The radius of the ice-cover was 150 km and its thickness 250 m. The duration of loading was 10 ka. Contour intervals are 0.2 mm/a.

negligible present day uplift-rates. On the other hand, if η is large and gives relaxation-times that are much larger than the time passed since the ice disintegration took place, the rebounding process is still under way but occurring slowly and therefore also giving rise to small uplift-rates. For fixed values of D and t_1 there will therefore be some value of η which gives maximum amounts of uplift-rate. Since decreasing D (all other parameters held fixed) has the effect of increasing t_r and shifting the maximum of $t_r(kD)$ to lower kD values there will also be some value of D which, for fixed values of η and t_1 , results in a maximum uplift-rate.

The most interesting fact about Figure 4 is that a range of combinations of η and D values that are in agreement with geological and geophysical findings obtained so far can be found to give uplift-rates comparable in magnitude with measured ones. Changing the radius R by ± 20 km does not affect this result. On the other hand can values for the rheological parameters which be found that are equally well in accordance with observations, but give much lower or even negligible uplift-rates. The result is therefore, with respect to the question of the cause of the observed vertical movements, inconclusive; depending on the parameters entering the model calculated uplift-rates comparable to as well as negligible with respect to the measured one's are obtained. It can only be said that at this level of modelling the possibility cannot be ruled out that a considerable if not even the dominant part of the observed uplift is caused by post-glacial isostatic rebound.

The uplift that has resulted since the load was removed at time $t = t_1$ is given by:

$$\delta v_z(r, t) = v_z(r, t) - v_z(r, t_1) \quad (11)$$

This quantity is referred to as the differential uplift. It is positive upwards. In Figure 5

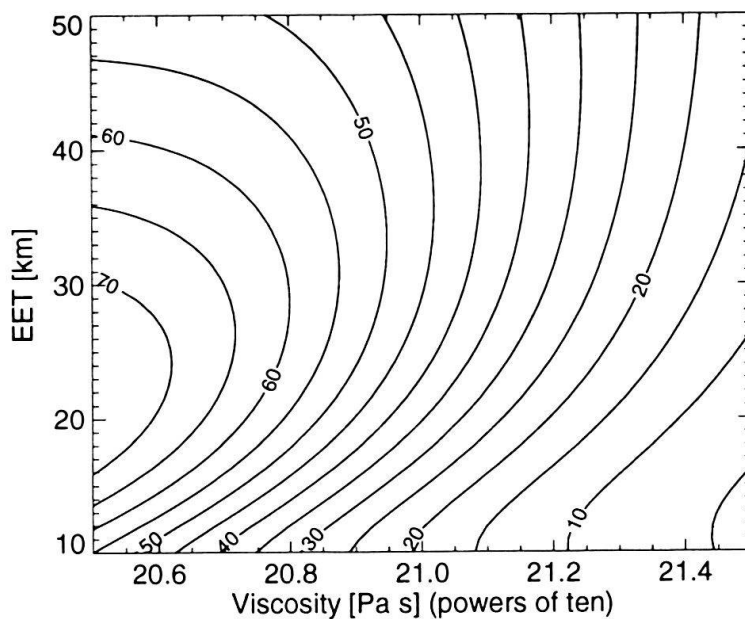


Fig. 5. Differential uplift in meters as a function of mantle viscosity η , and effective elastic thickness for a finite duration of loading.

All parameters are the same as in Fig. 4. Contour intervals are 5 m.

the differential uplift is given in meters as a function of η and D . Model parameters are the same as used for Figure 4 ($d = 250$ m, $R = 150$ km, $\rho_i = 920$ kg/m³, $\rho_v = 3250$ kg/m³, $\mu = 3.4 \times 10^{10}$ Pa, $t_1 = -13,000$ years, $t_1 - t_0 = 10,000$ years). The differential uplift is on the order of a few tens of meters. It is largest for low viscosity values where it approaches the maximum uplift possible.⁴ For these viscosity values the relaxation times are considerably less than $-t_1$ so that the rebound has already taken place long before now. For $\eta > 10^{21.4}$ Pa s only about 10% of the uplift has occurred. Notice that the uplift depends, as Eq. (7) shows, linearly on d .

5 Conclusions

An individual assessment of sufficient precision of the rheological parameters η and D could clarify the situation and give a definitive estimate of the contribution of the glacial isostatic rebound to the measured uplift-rate. In view of the uncertainties involved with the estimates done so far, a more promising approach seems, however, to be a true 2D-modelling where the spatial distribution of the Late Würm glaciation would be accounted for. The Alpine glaciation during Würm did not have the form of an ice sheet, and the form of the load used can only give an order of magnitude estimate. The magnitude of the low frequency components of the Hankel-transform of the ice load is relevant for the resulting uplift, since the crust acts basically as a low pass filter transmitting the low fre-

⁴ Because of the presence of the elastic plate the maximum possible uplift can be slightly larger at $r = 0$ than the isostatic value of $d \rho_i / \rho_v$.

quency components of the loading to the mantle while supporting elastically the high frequency components. It is not clear if the long wavelength spectrum of the load used is necessarily significantly different to the long wavelength spectrum of a more realistic load that takes into account the presence of valley glaciers with considerably larger thickness restrained to smaller areas.

The conclusion that a glacial isostasy can, for a range of rheological parameters in agreement with findings obtained so far, give rise to uplift-rates comparable in magnitude to the measured ones, stresses the need and can be seen as a justification for the development of a model with a more sophisticated load distribution. Preliminary work on such a model has already begun.

Acknowledgments

I wish to thank Dr. A. Iken, Dr. W. Haeberli, Dr. D. Werner, Dr. R. Freeman, Prof. H. Rötliberger and Prof. St. Mueller for useful comments that significantly improved the paper. I thank B. Nedela for preparing Figure 1.

REFERENCES

- CATHLES, L. M. 1975: The Viscosity of the Earth's Mantle. Princeton University Press, Princeton, N. J.
- CLOETINGH, S. & BANDA, E. 1992: Mechanical structure. In: *A Continent Revealed: The European Geotraverse* (Ed. by Freeman, R. & Mueller, S.), Cambridge University Press, 75–85.
- DAWSON, A. G. 1992: Ice Age Earth: Late Quaternary geology and climate. Physical Environment. Routledge.
- DE BEAULIEU, J.-L., MONJUVENT, G. & NICOU, G. 1991: Chronology of the Würmian glaciation in the French Alps: A survey and new hypotheses. In: *Klimageschichtliche Probleme der letzten 130 000 Jahre*. 1, B. Frenzel, Akademie der Wissenschaften und der Literatur, Mainz, 436–448.
- DRICOT, E., PETILLON, M. & SERET, G. 1991: When and why did glaciers grow or melt in the Vosges Mountains (France)? In: *Klimageschichtliche Probleme der letzten 130 000 Jahre*. 1, B. Frenzel, Akademie der Wissenschaften und der Literatur, Mainz, 363–375.
- ECKHARDT, P., FUNK, H. & LABHART, T. 1983: Postglaziale Krustenbewegungen an der Rhein-Rhône-Linie. *Vermessung, Photogrammetrie, Kulturtechnik* 2, 43–56.
- FJELDSKAAR, W. & CATHLES, L. 1991: Rheology of mantle and lithosphere inferred from post-glacial uplift in Fennoscandia. In: *Glacial Isostasy, Sea-Level and Mantle Rheology* (Ed. by Sabadini, R., Lambeck, K. & Boschi, E.) Kluwer Academic Publisher, 1–19.
- FUNK, H. & GUBLER, E. 1980: Höhenänderungen der Fixpunkte im Gotthard-Bahntunnel zwischen 1917 und 1977 und ihre Beziehung zur Geologie. *Eclogae geol. Helv.* 73, 583–592.
- GUBLER, E., ARCA, S., KAKKURI, J. & ZIPPELT, K. 1992: Recent vertical crustal movement. In: *A Continent Revealed: The European Geotraverse* (Ed. by Freeman, R. & Mueller, S.). Cambridge University Press.
- GUBLER, E., KAHLE, H.-G., KLINGELÉ, E., MUELLER, S. & OLIVIER, R. 1981: Recent crustal movements in Switzerland and their geophysical interpretation. *Tectonophysics* 71, 125–152.
- GUBLER, E., SCHNEIDER, D. & KELLERHALS, P. 1984: Bestimmung von rezenten Bewegungen der Erdkruste mit geodätischen Methoden. Technical Report 84–17, Nagra.
- GUDMUNDSSON, G. H. 1989: Modellrechnungen zu rezenten Alpenhebungen. Diploma thesis, Geophysical Institute ETH – Zürich.
- HAEBERLI, W. & PENZ, U. 1985: An attempt to reconstruct glaciological and climatological characteristics of 18 ka BP Ice Age glaciers in and around the Swiss Alps. *Z. Gletscherkd. und Glazialgeol.* 21, 351–361.
- HAEBERLI, W. & SCHLÜCHTER, C. 1987: Geological evidence to constrain modelling of the Late Pleistocene Rhône-gletscher (Switzerland). In: *The physical Basis of Ice Sheet Modelling*. Int. Assoc. Hydrol. Sci. Publ. 170, 333–346.
- HANTKE, R. 1980: *Eiszeitalter*, volume 1–3. Ott Verlag AG, Thun.
- HURFORD, A. J., FLISCH, M. & JÄGER, E. 1989: Unravelling the thermo-tectonic evolution of the Alps: a contribution from fission track analysis and mica dating. In: *Alpine Tectonics* (Ed. by Coward, M. P., Dietrich, M. P. & Park, R. G.) Geol. Soc. Spec. Publ. 45, 369–398.

- JÄCKLI, H. 1957: Gegenwartsgeologie des bündnerischen Rheingebietes. Beitr. geol. Schweiz. Geotechn. Ser. 36.
– 1970: Die Schweiz zur letzten Eiszeit. In: Atlas der Schweiz. Eidg. Landestopographie, Wabern–Bern.
- KAHLE, H.-G., MUELLER, S., KLINGELÉ, E., EGLOFF, R. & KISSLING, E. 1980: Recent dynamics, crustal structure and gravity in the Alps. In: *Earth Rheology, Isostasy and Eustasy* (Ed. by Möner, N.). Wiley, New York, N. Y., 377–388.
- KARATO, S. & WU, P. 1993: Rheology of the upper mantle: A synthesis. *Science* 260, 771–778.
- KARNER, G. D. & WATTS, A. B. 1983: Gravity anomalies and flexure of the lithosphere at mountain ranges. *J. Geophys. Res.* 83(B12), 10, 449–10, 477.
- KELLER, O. & KRAYSS, E. 1991: Der Eisaufbau des Rhein-Linth-Gletschers im Oberen Würm: Ein Modell. In: *Klimageschichtliche Probleme der letzten 130 000 Jahre*. 1. B. Frenzel, Akademie der Wissenschaften und der Literatur, Mainz, 422–433.
- KLINGELÉ, E. & KISSLING, E. 1982: Zum Konzept der Isostatischen Modelle in Gebirgen am Beispiel der Schweizer Alpen. In: *Geodätisch-geophysikalische Arbeiten in der Schweiz*, 35. Schweizerische Geodätische Kommission, 5–36.
- MCNUTT, M. K., DIAMENT, M. & KOGAN, M. G. 1988: Variations of elastic plate thickness at continental thrust belts. *J. Geophys. Res.* 93(B8), 8825–8838.
- MUELLER, S. 1989: Deep-reaching geodynamic processes in the Alps. In: *Alpine Tectonics* (Ed. by COWARD, M. P., DIETRICH, D. & PARK, R. G.) Spec. Publ. Geol. Soc. 45, 303–328.
- NAKIBOGLU, S. M. & LAMBECK, K. 1982: A study of the earth's response to surface loading with application to Lake Bonneville. *Geophys. J. R. ast. Soc.* 70, 577–620.
- OFFICER, C. B., SULLIVAN, J. M. & LYNCH, D. R. 1988: Glacial isostatic adjustment and mantle viscosity. *J. Geophys. Res.* 93, 6397–6409.
- SCHAEER, J.-P. & JEANRICHARD, F. 1974: Mouvements verticaux anciens et actuels dans les Alpes suisses. *Eclogae geol. Helv.* 67, 101–119.
- SCHAEER, J. P., REIMER, G. M. & WAGNER, G. A. 1975: Actual and ancient uplift rates in the Gotthard region, Swiss Alps: A comparison between precise levelling and fission-track apatite age. In: *Recent crustal movements* (Ed. by PARONI, N. & GREEN, R.). *Tectonophysics* 29, 293–300.
- SCHLÜCHTER, C. 1991: Fazies und Chronologie des letzteiszeitlichen Eisaufbaus im Alpenvorland der Schweiz. In: *Klimageschichtliche Probleme der letzten 130 000 Jahre*. 1. B. Frenzel, Akademie der Wissenschaften und der Literatur, Mainz, 401–407.
- SCHNEIDER, H. 1976: Über junge Krustenbewegungen in der voralpinen Landschaft zwischen dem südlichen Rheingraben und dem Bodensee. *Mitt. natf. Ges. Schaffhausen* 30, 1–99.
- SIGMUNDSSON, F. 1990: *Seigja jardar undir Íslandi*. Diploma thesis, Háskóli Íslands.
- SPAKMAN, W. 1990: Topographic images of the upper mantle below central Europe and the Mediterranean. *Terra Nova* 2, 542–553.
- WERNER, D. 1985: A two-dimensional geodynamic model for the southern segment of the EGT. In: *Second EGT Workshop – The southern Segment* (Ed. by GALSON, D. A. & MUELLER, S.). European Science Foundation, 65–69.

Manuscript received December 8, 1993

Revision accepted January 21, 1994

